which BSH and BPA were simultaneously combined, obtaining good tumor response on MRI, not only for the newly diagnosed malignant gliomas but also for the recurrent cases which had been initially treated by X-ray irradiation therapy (XRT). In our initial protocol, all of the patients received a combination of BSH (100 mg/kg) and BPA (250 mg/kg body weight) administered intravenously.

BNCT was carried out at the Kyoto University Research Reactor Institute (KURRI) using an epithermal neutron beam 12 and 1 h after the administration of BSH and BPA, respectively. This BNCT showed impressive radiographical shrinkage of the tumor mass, and improved the quality of life for even those patients with recurrent malignant gliomas, as described above and reported previously (Kawabata et al., 2003; Miyatake et al., 2005). We achieved a favorable survival benefit for newly diagnosed GB patients with this BNCT protocol, as described below. In the current modified protocol, we applied this BNCT followed by XRT to obtain a more favorable survival benefit for newly diagnosed GB (NDGB) patients. This study was based on experimental animal data showing that a significant therapeutic gain could be obtained when BNCT was combined with an X-ray boost (Barth et al., 2004).

2. Methods

Our BNCT protocol using both BPA and BSH simultaneously has been described previously (Kawabata et al., 2003). Our methods were as follows:

First, we started using epithermal neutrons instead of thermal neutrons to obtain good penetration for deep-seated lesions. Second, we simultaneously used two different boron compounds (BSH and BPA) with different accumulation mechanisms to the tumor cells (Yokoyama et al., 2006; Ono et al., 1999). Third, we utilized a dose simulation work station, the simulation environments for radiotherapy applications (SERA). Fourth, ^{18}F-labeled BPA-positron emission tomography (BPA-PET) was performed for the estimation of the boron compound accumulation prior to neutron irradiation (Imahori et al., 1998). Fifth, we filled the tumor removed cavity with air to obtain enough neutron flux, especially for the bottom of deep-seated tumors (Sakurai et al., 2006). Sixth, we developed a central shielding method with a lithium plate at the center of the irradiation field to obtain uniform neutron distribution and increase the neutron flux relatively at the periphery in the radiation field (Ono et al., 2000).

With these modifications, even patients with deep-seated tumors can be treated by BNCT without craniotomy with a short hospital stay. In the present study, the revised protocol was used as a new protocol as follows.

Twelve hours before the neutron irradiation, the patients were administered 100 mg/kg of BSH intravenously for 1 h. BPA of 700 mg/kg was infused continuously to the patients for 6 h before the irradiation, and they were positioned for neutron irradiation in the reactor (KUR or JRR-4 (Japan Atomic Energy Agency Research Reactor 4)). Just after termination of continuous BPA infusion for 6 h, neutrons were irradiated. We used the dose-planning workstation to calculate the radiation dose for tumors from the ^{18}F-labeled BPA-positron emission tomography data and blood ^{10}B concentrations obtained every 2 h after BSH administration. We used an epithermal neutron beam.

Following this, a 2 Gy daily fraction of XRT was applied, for a total of 20–30 Gy. The total dose of XRT was decided based on the BNCT dose for the normal brain. This protocol was approved by the Ethical Committee of Osaka Medical College and also by the Committee for Reactor Medicine in KURRI. In addition, the indication of BNCT for each candidate was discussed by the latter committee. In Protocol 1, we aimed to apply more than 30 Gy-Eq for gross tumor volume (GTV) and <12 Gy-Eq for normal brain, as BNCT. In Protocol 2, we aimed to apply more than 40 Gy-Eq for GTV and <15 Gy-Eq for normal brain.

Patient enrollment: In the current manuscript, we report the results only for NDGB patients. No chemotherapy was applied for any of the patients until the tumor progression was confirmed histologically or by BPA-PET. Survival time from histologically diagnosed GB was compared with the survival time of the institutional former series of GB patients who were treated by surgical removal followed by XRT and chemotherapy

Table 2

Group	*n*	MST	95% CI (months)	*P*-value (Log-rank test)
Without BNCT	27	10.3	(7.4–13.2)	
With BNCT	21	15.6	(12.2–23.9)	0.0035

See also Fig. 1.

Table 3

	Hazard ratio	95% CI	*P*-value
With BNCT (vs. control)	0.399	(0.206–0.746)	0.0038

See also Fig. 3.

Table 4

Group	*n*	MST	95% CI (months)	*P*-value (Log-rank test)
Historical control	27	10.3	(7.4–13.2)	
With BNCT only	10	14.1	(9.9–18.5)	0.0581
With BNCT plus XRT	11	23.5	(10.2–)	0.0103

See also Fig. 2.

Table 5

	Hazard ratio	95% CI	*P*-value
With BNCT (vs. control)	0.399	(0.206–0.746)	0.0038
BNCT+XRT (vs. control)	0.323	(0.128–0.710)	0.0040
BNCT+XRT (vs. BNCT only)	0.598	(0.0211–1.63)	0.3126

See also Fig. 3.

Table 1

Group	*n*	Mean ± SD (months)	Median (MST, months)	1 year (%)	2 years (%)
Without BNCT	27	12.3 ± 8.1	10.3	48.2	14.8
With BNCT	21	20.7 ± 13.1	15.6	76.2	25.0

See also Fig. 1.

(mainly ACNU) from 1990 to 2006 in Osaka Medical College. In this historical control group, all cases were operated on to aim for the maximum tumor removal, the same as for the cases of the BNCT group. The related Kaplan–Meier curves were calculated and the Log-rank test was used for statistical analysis. For the 21 patients who received BNCT, survival time was also compared with the corresponding recursive partitioning analysis (RPA) subclasses by the Radiation Therapy Oncology Group (RTOG) (Curran et al., 1993), as the international historical control. Based on this RTOG-RPA, GB was classified into four prognostic subgroups (classes III–VI), and the median survival for classes III, IV, V and VI were 17.9, 11.1, 8.9 and 4.6 months, respectively.

3. Results

Clinical results of the patients treated with BNCT in our studies are listed in Tables 1–5 and shown in Figs. 1–4.

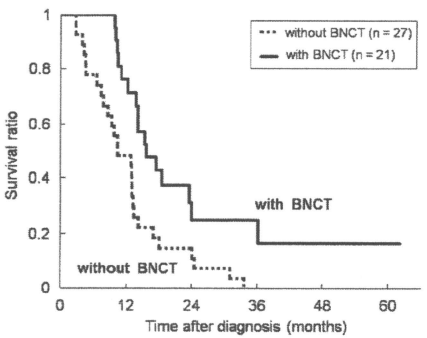

Fig. 1. Kaplan–Meier survivals. BNCT (with BNCT) vs. our historical control (without BNCT).

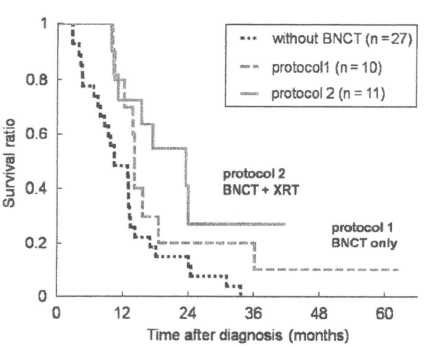

Fig. 2. Kaplan–Meier survivals. BNCT with XRT (protocol 2) vs. without XRT(protocol 1) and control (without BNCT).

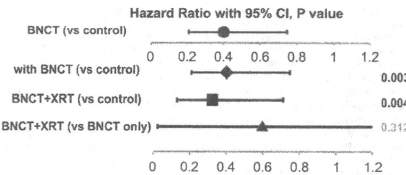

Fig. 3. Hazard ratios (Tables 3 and 4).

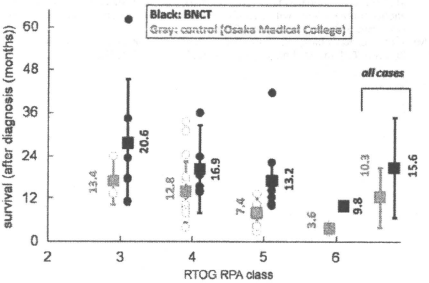

Fig. 4. Survival of the corresponding RPA subclasses by RTOG (Curran et al., 1993).

4. Conclusions

In conclusion, there were two major modifications to the current BNCT protocol (Protocol 2) in comparison with our former protocol (Protocol 1). The first modification is a longer term and a larger amount of BPA infusion, and the second is the additional application of XRT. Both modifications probably work synergistically and result in a more favorable survival benefit for GB patients.

Acknowledgments

Grant supports: Grants-in-Aid for Scientific Research for young researchers (B) (18791030 to S.K.), Grants-in-Aid for Scientific Research (B) (16390422 and 19390385 to S.-I.M.) from the Japanese Ministry of Education, Science and Culture. Grant-in-Aid for Scientific Research from the Ministry of Health, Labour and Welfare of Japan to S.-I.M. (P.I., Hideki Matsui), the Regional Science Promotion Program of the Japan Science and Technology Corporation, as well as by the "Second-term Comprehensive 10-Year Strategy for Cancer Control" of the Ministry of Health, Labor, and Welfare of Japan to S.-I.M., the Takeda Science Foundation for Osaka Medical College, Grant-in-Aid for Cancer Research from the Ministry of Education, Culture, Sports, Science, and Technology of Japan (12217065 to K.O.). We thank Yasuko Doi and Eriko Sugane for secretarial assistance.

References

Barth, R.F., Coderre, J.A., Vicente, M.G., Blue, T.E., 2005. Boron neutron capture therapy of cancer: current status and future prospects. Clin. Cancer Res. 11, 3987–4002.

Barth, R.F., Grecula, J.C., Yang, W., Rotaru, J.H., Nawrocky, M., Gupta, N., Albertson, B.J., Ferketich, A.K., Moeschberger, M.L., Coderre, J.A., Rofstad, E.K., 2004. Combination of boron neutron capture therapy and external beam radiotherapy for brain tumors. Int. J. Radiat. Oncol. Biol. Phys. 58, 267–277.

Curran Jr., W.J., Scott, C.B., Horton, J., Nelson, J.S., Weinstein, A.S., Fischbach, A.J., Chang, C.H., Rotman, M., Asbell, S.O., Krisch, R.E., Nelson, D.F., 1993. Recursive partitioning analysis of prognostic factors in three Radiation Therapy Oncology Group malignant glioma trials. J. Natl. Cancer Inst. 85, 704–710.

Doi, A., Kawabata, S., Iida, K., Yokoyama, K., Kajimoto, Y., Kuroiwa, T., Shirakawa, T., Kirihata, M., Kasaoka, S., Maruyama, K., Kumada, H., Sakurai, Y., Masunaga, S., Ono, K., Miyatake, S., 2008. Tumor-specific targeting of sodium borocaptate (BSH) to malignant glioma by transferrin-PEG liposomes: a modality for boron neutron capture therapy. J. Neuro-Oncol. 87, 287–294.

Imahori, Y., Ueda, S., Ohmori, Y., Sakae, K., Kusuki, T., Kobayashi, T., Takagaki, M., Ono, K., Ido, T., Fujii, R., 1998. Positron emission tomography-based boron neutron capture therapy using boronophenylalanine for high-grade gliomas: part I and II. Clin. Cancer Res. 4, 1825–1841.

Kawabata, S., Miyatake, S., Kajimoto, Y., Kuroda, Y., Kuroiwa, T., Imahori, Y., Kirihata, M., Sakurai, Y., Kobayashi, T., Ono, K., 2003. The early successful treatment of glioblastoma patients with modified boron neutron capture therapy. Report of two cases. J Neuro-Oncol. 65, 159–165.

Miyatake, S., Kawabata, S., Kajimoto, Y., Aoki, A., Yokoyama, K., Yamada, M., Kuroiwa, T., Tsuji, M., Imahori, Y., Kirihata, M., Sakurai, Y., Masunaga, S., Nagata, K., Maruhashi, A., Ono, K., 2005. Modified boron neutron capture therapy for malignant gliomas performed using epithermal neutron and two boron compounds with different accumulation mechanisms: an efficacy study based on findings on neuroimages. J. Neurosurg. 103, 1000–1009.

Ono, K., Masunaga, S., Suzuki, M., Kinashi, Y., Takagaki, M., Akaboshi, M., 1999. The combined effect of boronophenylalanine and borocaptate in boron neutron capture therapy for SCCVII tumors in mice. Int. J. Radiat. Oncol. Biol. Phys. 43, 431–436.

Ono, K., Sakurai, Y., Masunaga, S., Kinashi, Y., Takagaki, M., Kobayashi, T., 2000. Improvement of B-10 dose distribution in water phantom irradiated with epithermal neutron beam and its assessment by colony formation assay. In: Program and Abstracts of the Ninth International Symposium on Neutron Capture Therapy for Cancer. Kyoto University Research Reactor Institute, Osaka, Japan, pp. 197–198.

Sakurai, Y., Ono, K., Miyatake, S., Maruhashi, A., 2006. Improvement effect on the depth-dose distribution by CSF drainage and air infusion of a tumour-removed cavity in boron neutron capture therapy for malignant brain tumours. Phys. Med. Biol. 51, 1173–1183.

Yokoyama, K., Miyatake, S., Kajimoto, Y., Kawabata, S., Doi, A., Yoshida, T., Asano, T., Kirihata, M., Ono, K., Kuroiwa, T., 2006. Pharmacokinetic study of BSH and BPA in simultaneous use for BNCT. J. Neuro-Oncol. 78, 227–232.

Applied Radiation and Isotopes 67 (2009) S47–S49

Contents lists available at ScienceDirect

Applied Radiation and Isotopes

journal homepage: www.elsevier.com/locate/apradiso

Boron neutron capture therapy for recurrent oral cancer and metastasis of cervical lymph node

Y. Kimura [a,*], Y. Ariyoshi [a], M. Shimahara [a], S. Miyatake [b], S. Kawabata [b], K. Ono [c], M. Suzuki [c], A. Maruhashi [d]

[a] Department of Dentistry and Oral Surgery, Division of Medicine for Function and Morphology of Sensory Organs, Osaka Medical College, 2-7 Daigaku-machi Takatsuki City, Osaka, Japan
[b] Department of Neurosurgery, Division of Surgery, Osaka Medical College, 2-7 Daigaku-machi Takatsuki City, Osaka, Japan
[c] Particle Radiation Oncology Research Center, Kyoto University, Kumatori-cho, Sennan-gun, Osaka, Japan
[d] Medical Physics, Department of Radiation Life Sciences, Research Reactor Institute, Kyoto University, Kumatori-cho, Sennan-gun, Osaka, Japan

ARTICLE INFO

Keywords:
Boron neutron capture therapy (BNCT)
Oral cancer
Boronophenylalanine (BPA)

ABSTRACT

We treated 6 patients with recurrent oral cancer and metastasis to the cervical lymph nodes after conventional treatments in 5 and non-conventional in 1 using BNCT, and herein report our results. The clinical response in our patients ranged from CR to PD. In 5 cases, spontaneous pain decreased immediately after BNCT. Three of the 6 are alive at the time of writing and we found that BNCT contributed to QOL improvement in all.

1. Introduction

A radical operation for recurrent and progressive oral cancer is functionally and aesthetically difficult, due to anatomical complexity, while chemotherapy or radiotherapy do not generally result in a radical cure. Oral cancer causes intense pain and makes eating by mouth difficult when advanced, thus markedly reducing patient quality of life (QOL). We have performed boron neutron capture therapy (BNCT) in 6 patients with recurrent oral cancer since introducing the method at our institution in 2005. BNCT is a type of tumor-selective radiotherapy , in which cancer cells are destroyed by alpha and ^{7}Li particles generated by the nuclear reaction between boron (^{10}B) uptake in the tumor and thermal or epithermal neutron (Coderre and Morris, 1999). It has excellent clinical characteristics and is superior in regard to local control effects. Moreover, pain is controlled with the therapy, while serious mucositis and osteomyelitis of the jaw bone do not develop.

2. Patients

We treated 6 patients (3 males and 3 females) with recurrent oral cancer and metastasis to the cervical lymph nodes. Each had suffered a recurrence after conventional therapy, such as surgery, chemotherapy, or radiotherapy, although 1 case was not treated by conventional treatment and included in the present analysis (Table 1).

Histopathological findings revealed 2 cases of squamous cell carcinoma, 2 cases of adenocarcinoma, 1 case of mucoepidermoid carcinoma, and 1 case of melanoma. Prior to BNCT, informed consent was obtained from all of the subjects, and the study protocol was approved by the ethical committees of Osaka Medical College and Kyoto University Research Reactor Institute (KURRI).

3. Methods

The distribution of boronophenylalanine (BPA), used as a boron compound, in the tumor and surrounding healthy tissue can be visualized using a two-dimensional image obtained by an ^{18}F-BPA-PET examination, which was conducted to evaluate BPA uptake in the tumors in all of the present cases (Imahori et al., 1998) (Fig. 1).

From those results, the difference in boron concentration (T/N ratio) between the tumor and normal tissues was determined. For the boron compound, BPA at 500 mg/kg of body weight was administered intravenously by drip infusion starting from 2 to 3 h before and during irradiation. In Case 3, sodium borocaptate (BSH) at 2 g/body weight was used concomitantly. For neutron irradiation, a research reactor with an output of 5 MW located at KURRI was utilized. We used the BNCT exposure dose planning system SERA for estimating and evaluating the neutron flux distribution, as well as the distribution of the absorbed dose of epithermal neutrons high-speed neutrons and gamma rays. A gold wire set

* Corresponding author. Tel.: +81 72 683 1221; fax: +81 72 681 3723.
E-mail address: ora018@poh.osaka-med.ac.jp (Y. Kimura).

0969-8043/$ - see front matter Crown Copyright © 2009 Published by Elsevier Ltd. All rights reserved.
doi:10.1016/j.apradiso.2009.03.019

Table 1
Characteristics of patients.

Case	Age/sex	Location	Histopathological diagnosis	Previous treatment	Symptoms
1	41/M	Cervical lymph node	SqCC	S, CH, Ra	ED, Pa
2	32/M	Cervical lymph node	Melanoma	S, CH	
3	82/F	Upper lip	AC	Th	ED, Pa
4	57/M	Maxilla	SqCC	S, CH, Ra	ED, Pa
5	67/F	Maxilla	MC	S, CH, Ra	ED, Pa, B
6	69/F	Maxilla	AC	S, CH, Ra	ED, Pa

SqCC: squamous cell carcinoma; AC: adenocarcinoma; MC: mucoepidermoid carcinoma; S: surgery; CH: chemotherapy; Ra: conventional radiotherapy; Th: thermotherapy; ED: eating disorder; Pa: pain; B: bleeding.

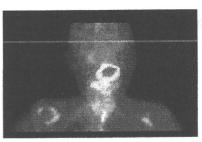

Fig. 1. ^{18}F-BPA-PET examination can visualize the distribution of boronophenylalanine (BPA).

used for measurement was removed at 10 min after the start of irradiation to evaluate epithermal neutron flux on a collimator Bi surface at a point 25 cm from the center and at the center of the irradiation field on the affected surface. The full-time exposure dose on the surface adjacent to the affected portion was determined by measuring neutron fluence (nvt) using gold and manganese wires. The absorbed dose of gamma rays was measured using a TLD (BeO), with the gold wire and TLD set in the vicinity of the center of the affected surface. The ^{10}B concentration in blood was determined by collecting venous samples every 30 min after BPA administration until just before irradiation, as well as after irradiation for prompt gamma radiation measurement.

Following BNCT, the tumor regression, adverse side effects, survival time, and subjective symptoms were recorded. For evaluating adverse side effects, the Common Terminology Criteria for Adverse Events v3.0 (CTCAE v3.0) was used. Tumor regression was evaluated by CT and MR imaging.

4. Results

T/*N* ratios calculated on the basis of the ^{18}F-BPA-PET results ranged from 1.9 to 4.0. The maximum dose to the tumor (Gy-Eq) was 20.1–39.1 Gy-Eq and the minimum 9.12–31.9 Gy-Eq, while the dose to the oral mucosa was 9.03–15.7 Gy-Eq and to the skin was 2.81–7.64 Gy-Eq (Table 2).

Tumor reduction was rated as PR in 4 cases, while 1 case was CR and 1 was PD. Notably, in Case 2 with metastasis to the lymph nodes that was within the BNCT irradiation range, the reduction was rated as CR (Fig. 2).

As for clinical improvement, pain was alleviated in all 5 cases in which pain was observed before the study and difficulty eating was improved in each of those. Especially in Cases 1 and 4, the patients, who were forced to stay in the hospital due to pain and difficulty eating, were temporarily discharged after BNCT. In Case 5, bleeding from the tumor was reduced. For adverse side effects, mucositis, fatigue, alopecia, impaired taste, and pharyngeal edema were observed, although none was severe. Neither myelosuppression nor osteomyelitis of the jaw bone was observed.

Three of the 6 patients survived for a range of 23–29 months after the final BNCT. In Case 1, a tumor in the cervical lymph node was markedly reduced after BNCT, then later became enlarged, which led to death from aspiration pneumonia 4 months later. In Case 2, a tumor in the cervical lymph node was reduced to the level of CR and the patient died from lung metastasis 16 months later. In Case 4, the tumor enlarged after therapy and the patient died 13 months later. The other 3 patients were alive at the time of writing (Table 3).

5. Discussion

^{10}B, a stable isotope of boron that captures a low-energy neutron, splits off into alpha-particles and Li atomic nuclei. Their ranges are approximately 9 and 4 μ, respectively, which are equivalent to the size of a tumor cell. BNCT makes use of the reaction and selectively destroys tumor cells by causing low-energy neutrons to react with ^{10}B preliminarily uptaken by tumor cells. The therapy was performed for the first time by Farr et al. (1954) for glioblastoma multiforme, after which Kato et al. (2004) began to utilize it for head and neck cancer that had relapsed after initial treatment, and reported 11 cases.

Oral cancer in the early stage of T1 or T2 is frequently treated with surgery. However, it is difficult to obtain a radical cure for progressive or recurrent cancer after completion of the initial treatment, even if multimodal approaches such as surgery, radiotherapy, and chemotherapy are used. Accordingly, improvements in therapeutic performance are not encouraging, unless some new therapeutic strategies are developed. We have been performing BNCT treatment for recurrent cancer that relapsed after completion of initial treatment, including surgery, chemotherapy, conventional radiation therapy, and thermotherapy since 2005.

In BNCT, tumor cells take up boron and then are selectively destroyed. This reduces the impact on normal cells, and adverse effects can be alleviated. In the 6 cases described in this report, myelosuppression and skin lesions, normally seen with conventional radiation therapy, were not observed. Notably, osteomyelitis of the maxillary bone, which often develops after conventional radiation therapy for oral cancer, was not seen. These findings are extremely significant clinically, as osteomyelitis of the jaw bone after radiation therapy can induce infection and fracture, which causes difficulty in dealing with the intense pain. In addition, the mucositis and fatigue observed in most cases were mild and rated as grade 2 or lower.

As for clinical response, 4 cases were rated as PR, with 1 case each as PD and CR. Case 2 is quite interesting. In this patient, BNCT was performed for metastasis to the cervical lymph nodes after initial surgery and chemotherapy for melanoma in the maxillary gingiva. With melanoma, the presence of metastasis to the lymph nodes affects the prognosis, as the 5-year survival rate is 39% for

Table 2
Parameters of BNCT.

Case	Boron compound	T/N ratio of ^{18}F-BPA	Dose (Gy-Eq)			
			Skin surface	Oral mucosa	Tumor peak	Tumor minimum
1	1BPA	4.0	4.93	14.4	39.1	15.0
	2BPA		2.85	9.52	25.5	10.3
2	1BPA	1.9	4.6	14.4	20.1	15.7
	2BPA+BSH		7.64	15.7	35.5	29.0
3	1BPA	3.2	4.1	15.4	34.6	31.9
	BPA		3.59	12.9	28.8	27.9
4	1BPA	3.4	3.22	9.13	21.6	9.12
	BPA		2.81	9.03	21.1	20.4
5	1BPA	2.2	3.74	15.3	24.8	22.0
6	1BPA	2.4	7.2	15.0	38.3	17.1

Fig. 2. Case2: Left: CT image taken before BNCT. Right: CT image taken after BNCT. Metastasis of the lymph node reduced completely.

Table 3
Clinical results.

Case	Clinical response I	Clinical response II	Adverse side effects (grade)	Outcome (duration after BNCT)
1	PD	DP, IE	M (2), F (1)	Died (4 months)
2	CR		M (3), F (1), AL (1), I (1), PE (2)	Died (16 months)
3	PR	DP, IE	M (2), F (1)	AD
4	PR	DP, IE	M (1), F (1)	Died (13 months)
5	PR	DP, IE, DB	M (1), AL (1)	AD
6	PR	DP, IE	M (2), F (1)	AD

DP: decreased pain; IE: improved eating; DB: decreased bleeding; M: Mucositis; F: fatigue; AL: alopecia; I: impaired taste; PE: pharyngeal edema; AD: alive with disease.

cases with metastasis to the lymph nodes, whereas it is 80% for negative cases (Goldsmith, 1970). Our patient died from lung metastasis at 16 months after BNCT. However, the metastasis had completely disappeared from the cervical lymph nodes where BNCT was administered, suggesting the effectiveness of BNCT for highly malignant melanoma.

The mouth has a variety of functions such as eating and talking, as well as aesthetic qualities. These functions are disturbed easily as oral cancer progresses, while QOL is severely affected when pain is added. BNCT is effective not only for reducing the size of the tumor, but also in controlling pain and decreasing bleeding, thus contributing to QOL improvement. The most important goal of this therapy is tumor regression, with complete cure and reintegration of the patient into normal life. However, this has yet to be achieved.

The success or failure of BNCT is dependent on whether the ^{10}B compound can be selectively taken up by the nuclei of the tumor cells. Miyatake et al. (2005) reported that the combination of BPA and BSH increased the ^{10}B concentration in patients with malignant brain tumors. In Case 2, we aimed at the cervical lymph nodes as the target and used BPA as the boron compound during the first irradiation. However, since the tumor peak dose was low at 20.1 Gy-Eq, we used BHS concomitantly during the second irradiation. As a result, the tumor peak dose elevated to 35.5 Gy-Eq and the target lymph nodes attained CR.

Although the number of cases presented was small, all of our cases were patients with recurrent or metastatic cancer after the completion of an initial treatment we considered that these patients might face difficulties not only with the therapeutic effect on the tumors, but also QOL improvement, if treated by conventional treatment. Although BNCT could not bring about a complete cure, it greatly improved the QOL of each patient without causing serious adverse side effects. For BNCT for the oral and maxillofacial region, additional detailed studies are necessary in regard to the method of fixing and positioning the patient. In a future study, we intend to investigate the detailed clinical and basic requirements to develop a more effective treatment method.

References

Coderre, J.A., Morris, G.M., 1999. The radiation biology of boron neutron capture therapy. Radiat. Res. 151, 1–18.

Farr, L.E., Sweet, W.H., Robertson, J.S., et al., 1954. Neutron capture therapy with boron in the treatment of glioblastoma multiforme. Am. J. Roentogenol. 71, 279.

Goldsmith, H.S., 1970. Prognostic significance of lymphnode dissection in the treatment of malignant melanoma. Cancer 26, 606–609.

Imahori, Y., Ueda, S., Omori, Y., et al., 1998. Fluorine-18-labeled fluoroboronphenylalanine PET in patients with glioma. J. Nucl. Med. 39, 325–333.

Kato, I., Ono, K., Sakurai, Y., et al., 2004. Effectiveness of BNCT for recurrent head and neck malignancies. Appl. Radiat. Isot. 61 (5), 1069–1073.

Miyatake, S., Kawabata, S., Kajimoto, Y., et al., 2005. Modified boron neutron capture therapy for malignant gliomas performed using epithermal neutron and two boron compounds with different accumulation mechanisms. J. Neurosurg., 1000–1009.

Applied Radiation and Isotopes 67 (2009) S22–S24

Contents lists available at ScienceDirect

Applied Radiation and Isotopes

journal homepage: www.elsevier.com/locate/apradiso

Survival benefit of boron neutron capture therapy for recurrent malignant gliomas

Shin-Ichi Miyatake [a,*], Shinji Kawabata [a], Kunio Yokoyama [a], Toshihiko Kuroiwa [a], Hiroyuki Michiue [b], Yoshinori Sakurai [c], Hiroaki Kumada [d], Minoru Suzuki [c], Akira Maruhashi [c], Mitsunori Kirihata [e], Koji Onoc [c]

[a] Department of Neurosurgery, Osaka Medical College, 2-7 Daigaku-machi, Takatsuki City, Osaka 569-8686, Japan
[b] Department of Neurosurgery, Okayama University, 2-5-1 Shikata-cho, Okayama 700-8558, Japan
[c] Particle Radiation Oncology Research Center, Research Reactor Institute, Kyoto University, Kumatori 590-0494, Japan
[d] Department of Research Reactor and Tandem Accelerator, Nuclear Science Institute, Japan Atomic Energy Agency, Tokai 319-1184, Japan
[e] Department of Agriculture, Osaka Prefectural University, Sakai 599-8531, Japan

ARTICLE INFO

Keywords:
Boronophenylalanine PET
Glioblastoma
Malignant glioma
Recursive partitioning analysis (RPA)

ABSTRACT

We have applied boron neutron capture therapy (BNCT) to malignant brain tumors. Here we evaluated the survival benefit of BNCT for recurrent malignant glioma (MG). Since 2002, we have treated 22 cases of recurrent MG with BNCT. Survival time was analyzed with special reference to recursive partitioning analysis (RPA) classification, by Carson et al. Median survival times (MSTs) after BNCT for all patients and for glioblastoma as on-study histology at recurrence was 10.8 months ($n = 22$; 95% CI, 7.3–12.8 months) and 9.6 months ($n = 19$; 95% CI, 6.9–11.4 months), respectively. In our study, MST for the high-risk RPA classes was 9.1 months ($n = 11$; 95% CI, 4.4–11.0 months). By contrast, the original journal data showed that the MST of the same RPA classes was 4.4 months ($n = 129$; 95% CI, 3.6–5.4 months). BNCT showed a survival benefit for recurrent MG, especially in the high-risk group.

1. Introduction

We have applied a form of tumor-selective particle radiation, boron neutron capture therapy (BNCT), for malignant gliomas (MGs) and malignant meningiomas.

The prognosis of recurrent MGs, especially glioblastoma multiforme (GBM) is poor. We reported the effectiveness of BNCT on neuroimages for MGs, and recently reported the survival benefit of BNCT for newly diagnosed MGs (submitted for publication). Unfortunately, the standard treatment for recurrent MG has not yet been established. Therefore, evaluation of the survival benefit of BNCT for recurrent MGs is difficult. To evaluate this objectively, we adopted the recursive partitioning analysis (RPA) classification for recurrent MG advocated by Carson et al. in a 2007 article in the *Journal of Clinical Oncology*, in which the results of 10 recent protocols of phase-1 and -2 trials applied by the New Approaches to Brain Tumor Therapy CNS Consortium (NABTT) for recurrent MG were summarized (Carson et al., 2007). They included six systemic treatment and four local treatment trials. Originally this RPA classification was not aimed at the evaluation of the effectiveness of each trial for recurrent MG; however, this RPA classification gave us a uniform background and median survival time (MST) for each recurrent MG-type patient at the time of recurrence. So we classified our recurrent MG patients treated by BNCT and compared their survival to the MSTs presented in the above journal.

2. Patients and methods

2.1. Patient enrollment

From 2002 to 2007 we treated a total of 22 cases of recurrent MG using BNCT. Our eligibility criteria for this trial were as follows: (1) age 15 years or older; (2) histologically proven supratentorial MG (GBM, AA, AO, or anaplastic oligodendroglioma, as on-study histology) that had proved to be progressive or recurrent after radiation therapy; (3) depth of the tumor from scalp less than 6 cm (if the lesion is deeper than 6 cm from the scalp, partial removal or cyst evacuation was applied to fit this criteria, see below); (4) no cerebrospinal fluid (CSF) dissemination at recurrence; (5) estimated life expectancy longer than three months, not pregnant or breast feeding, and having a KPS score of 60 or greater.

* Corresponding author.
E-mail address: neu070@poh.osaka-med.ac.jp (S.-I. Miyatake).

0969-8043/$ - see front matter © 2009 Elsevier Ltd. All rights reserved.
doi:10.1016/j.apradiso.2009.03.032

2.2. Clinical regimen of BNCT

In protocol 1, the patients were administered 100 mg/kg of sodium borocaptate (BSH) and 250 mg/kg of BPA for one hour intravenously 12 h prior and just prior to neutron irradiation, respectively. In protocol 2, the patients were administered 100 mg/kg of BSH intravenously for 1 h, 12 h prior to neutron irradiation and 700 mg/kg of BPA continuously for 6 h before the irradiation. In both protocols, the neutron irradiation time was determined not to exceed 13 Gy-Eq to the normal brain by simulation.

2.3. Patient characteristics

The patients' age is 51 (15–67) (median and range), gross tumor volume (GTV) is 42 ml (4.1–64.5) (median and range). In 12 cases surgery was applied before BNCT, as a form of cyst evacuation or partial tumor removal to make a cavity to establish an Ommaya reservoir as described above. Ten cases were administered TMZ, three before the relapse and seven after BNCT.

2.4. RPA classification

To objectively evaluate the survival benefit of BNCT for recurrent MG, we classified our BNCT cases according to the RPA classification advocated in some journals (Carson et al., 2007). These classifications can be summarized as follows: class 1, not GBM (initial histology), KPS $\geqslant$ 80, frontal (tumor location); RPA class 2, not GBM, KPS $\geqslant$ 80, not frontal; RPA class 3, not GBM, KPS $\leqslant$ 70; RPA class 4, GBM, age $\leqslant$ 50, KPS $\geqslant$ 90; RPA class 5, GBM, age $\leqslant$ 50, 60 $\leqslant$ KPS $\leqslant$ 80; RPA class 6, GBM, age $\geqslant$ 50, no steroid use; RPA class 7, GBM, age $\geqslant$ 50, steroid use.

3. Results

3.1. Survival after BNCT and after diagnosis

Survival after BNCT ($n = 22$) and that from initial GBM diagnosis ($n = 19$, on-study histology as GBM) are shown in Fig. 1. MST after BNCT for all patients ($n = 22$) was 10.8 months (95% CI, 7.3–12.8 months). MST after BNCT for GBM cases as on-study histology at recurrence ($n = 19$) was 9.6 months (95% CI, 6.9–11.4 months). MST after initial GBM diagnosis ($n = 19$) was 19.1 months (95%CI, 11.6–23.0 months).

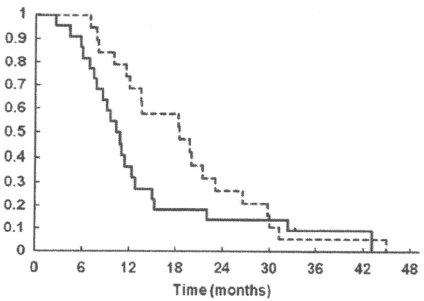

Fig. 1. Kaplan-Meier survival curves for recurrent MG cases treated by BNCT. The continuous line shows the survival of all patients after BNCT ($n = 22$). The broken line shows the survival of GBM (on-site histology) after diagnosis of GBM ($n = 19$).

Table 1
Comparison of NABTT trials and our BNCT series.

	All patients			RPA 3+7		
	MST	95% CI	Number in series	MST	95% CI	Number in series
NABTT	7.0	6.2–8.0	$n = 310$	4.4	3.6–5.4	$n = 129$
BNCT	10.8	7.3–12.8	$n = 22$	9.1	4.4–11.0	$n = 11$

3.2. Survival with special reference to RPA classes

The MSTs (months) of our BNCT cases classified according to RPA classes are shown here and compared in each case with the values from Carson et al.: class 1 ($n = 2$): 32.6 versus 25.7 (Carson et al.), class 2 ($n = 4$): 23.7 versus 17.2, class 3 ($n = 5$): 9.1 versus 3.8, class 4 ($n = 3$): 10.2 versus 10.4, class 5 ($n = 2$): 8.5 versus 6.4, class 7 ($n = 6$): 9.8 versus 4.9. The tendencies in patient survival of our cases after BNCT were very similar to those of the original report in terms of RPA classification. Since our cases were so limited in number, we joined the worst prognosis classes (classes 3 and 7) together into one class. The MST of our cases in this combined class was 9.1 months ($n = 11$; 95% CI, 4.4–11.0 months), while that in Carson et al. was 4.4 months ($n = 129$; 95% CI, 3.6–5.4 months) (Table 1).

4. Discussion

Here we reported the survival benefit of BNCT for recurrent MG cases, mainly GBM. The MST after BNCT for GBM cases as on-study histology at recurrence ($n = 19$) was 9.6 months (95% CI, 6.9–11.4 months). In the literature, we found a summary of a large series of 8 phase-2 trials of chemotherapies for recurrent GBM cases (Wong et al., 1999). In this report, the authors mentioned the MST of GBM after relapse as 25 weeks (5.8 months; 95% CI, 21–28 weeks, 4.9–6.5 months; $n = 225$). In comparison with this result, our data for the survival benefit of BNCT in recurrent GBM was not bad.

As to BNCT for recurrent GBM, two small series have been reported in the literature. A Swedish group and a Finnish group reported that MSTs for recurrent GBM after BNCT were 8.7 ($n = 12$) (Pellettieri et al., 2008) and 7.5 months ($n = 7$), respectively. Our data in the current report is almost equal to or somewhat better than the findings in these reports.

Kaplan-Meyer analysis in Fig. 1 showed that MST after BNCT for all patients ($n = 22$) was 10.8 months (95% CI, 7.3–12.8 months). We are not sure whether this result is reliable, as this is the result of a small series from a single institute. To evaluate this result as objectively as possible, we applied RPA to our cases as advocated in the literature (Carson et al., 2007). Inclusion criteria for our trial and the 10 NABTT phase-1 and -2 trials reported in Carson et al. were not very different. Our case numbers for each RPA class were so limited, however, that the MST of our cases in each RPA class were relatively better in comparison with original NABTT results, as listed above. In the original article, RPA class 3 (not GBM, KPS $\leqslant$ 70) and class 7 (GBM, age $\geqslant$ 50, steroid use) showed extremely poor prognosis. The MST of our combined classes 3 and 7 cases was 9.1 months ($n = 11$; 95% CI, 4.4–11.0 months), while that in the original article was 4.4 months ($n = 129$; 95% CI, 3.6–5.4 months) (Table 1). We cannot know whether our current MST data is significantly better than that of each NABTT trial because their raw data were not available. But at least, BNCT

showed a good survival benefit even for the highest-risk group, RPA classes 3 and 7.

In our 22 cases, we used TMZ in 10 cases, before BNCT in three cases and after BNCT in 7. For the former three cases, TMZ could not control the tumor growth and methylation-specific PCR showed an unmethylated O6-methylguanine DNA methyltransferase (MGMT) promoter (data not shown). We stopped the administration of TMZ after BNCT as we judged TMZ was not efficacious for these three cases. Among the latter seven cases, only two (cases 1 and 2, both classified as RPA class 1) showed methylated promoter status for MGMT, with good prognoses. For the other five cases, we were not sure of the MGMT expression status of the tumor. In the high-risk group in our series (RPA classes 3 and 7), three cases were administered TMZ after BNCT. Among them, two cases showed a relatively shorter survival after BNCT. We do not deny the meaning of TMZ use at relapse; however, in our series for this high-risk group, the survival benefit of TMZ was limited. In the literature, TMZ has actually shown modest survival benefit at relapse of recurrent GBM reported only 5.4 months prolongation as MST with TMZ at relapse in the report. (Brada et al., 2001).

There are several reports with relatively good results for recurrent MG, with an MST of around 10 months after the stereotactic radiosurgery (SRS) or stereotactic radiotherapy (SRT) at relapse. However, there was big difference in GTV at the relapse between these SRS or SRT cases and ours. The median GTV of the former two was 10.1 and 12.7 ml, while the median GTV of our cases was 42.0 ml. There might also be a difference as to performance status or age between the SRS or SRT reports and our cases. The result of re-irradiation for recurrent GBM was poor. The MST of this report was 26 weeks after the treatment. In addition, BNCT can be applied in only one day. Taken together, BNCT could be one of the promising radiation treatment options for recurrent MG at relapse.

We lost many cases of recurrent MGs after BNCT by CSF dissemination, as we reported (in preparation). In other words, local control by BNCT for even recurrent MG was fairly good. There was a tendency for CSF dissemination to occur in relatively long-term survivors from diagnosis (data not shown). On the other hand, a major problem in BNCT for recurrent MG was the occurrence of radiation necrosis (RN). We experienced RN by BNCT especially for recurrent MG, because the patients had been treated by radiotherapy prior to BNCT. Although BNCT is cell-selective particle radiation, some particle dose is inevitably absorbed by the normal brain tissue. Most of RN could be controlled with medical or surgical treatments as above; however, we lost three cases by RN in our series. Preventive medical treatments such as by anticoagulants or by vitamin E must be considered after BNCT, especially for recurrent cases. This is not mentioned in other BNCT reports for recurrent MG; however, it should be seriously considered. In Swedish reports of BNCT for recurrent GBM, the authors mentioned a median time to tumor progression (TP) of six months after BNCT, but there was no statement as to how TP was judged in their report. It is very difficult to differentiate RN and TP on MRI, especially with high-dose radiation treatment. So we did not apply the analysis of time to tumor progression in our series. Especially for recurrent cases, if we increase the minimum tumor dose by BNCT, the incidence of RN probably increases, as discussed here. Therefore, it is very difficult to elucidate the most suitable dose of BNCT at relapse. Regardless, RN is a serious problem to be overcome in the field of BNCT.

XRT plus concomitant TMZ (Stupp's regimen) has been the global standard so far for newly diagnosed GBM (Stupp et al., 2005). Pellettieri et al. reported that BNCT at relapse after Stupp's regimen might be the best treatment of GBM. Also in our series BNCT at relapse showed a good MST after the initial GBM diagnosis of 19.1 months ($n = 19$; 95%CI, 11.6–23.0 months). But it cannot be concluded so easily that BNCT at relapse after Stupp's regimen is the best for the treatment of GBM because 19 cases in our series were referred to our institute at relapse with a significant interval after initial treatments. This interval might prolong the survival after initial GBM diagnosis at a glance.

5. Conclusions

The RPA classification advocated by Carson et al. predicted the patient survival trends of our BNCT series; however, BNCT showed the most prominent survival benefit in the high-risk group (RPA classes 3 and 7).

References

Brada, M., Hoang-Xuan, K., Rampling, R., Dietrich, P.Y., Dirix, L.Y., Macdonald, D., et al., 2001. Multicenter phase II trial of temozolomide in patients with glioblastoma multiforme at first relapse. Ann. Oncol. 12, 259–266.

Carson, K.A., Grossman, S.A., Fisher, J.D., Shaw, E.G., 2007. Prognostic factors for survival in adult patients with recurrent glioma enrolled onto the new approaches to brain tumor therapy CNS consortium phase I and II clinical trials. J. Clin. Oncol. 25, 2601–2606.

Pellettieri, L., Stenstam, B.H., Rezaei, A., Giusti, V., Skold, K., 2008. An investigation of boron neutron capture therapy for recurrent glioblastoma multiforme. Acta Neurol. Scand. 117, 191–197.

Stupp, R., Mason, W.P., van den Bent, M.J., Weller, M., Fisher, B., Taphoorn, M.J., et al., 2005. Radiotherapy plus concomitant and adjuvant temozolomide for glioblastoma. N. Engl. J. Med. 352, 987–996.

Wong, E.T., Hess, K.R., Gleason, M.J., Jaeckle, K.A., Kyritsis, A.P., Prados, M.D., et al., 1999. Outcomes and prognostic factors in recurrent glioma patients enrolled onto phase II clinical trials. J. Clin. Oncol. 17, 2572–2578.

Applied Radiation and Isotopes 67 (2009) S258–S261

Contents lists available at ScienceDirect

Applied Radiation and Isotopes

journal homepage: www.elsevier.com/locate/apradiso

Improvement of dose distribution in phantom by using epithermal neutron source based on the Be(p,n) reaction using a 30 MeV proton cyclotron accelerator

H. Tanaka [a,*], Y. Sakurai [a], M. Suzuki [a], T. Takata [a], S. Masunaga [a], Y. Kinashi [a], G. Kashino [a], Y. Liu [a], T. Mitsumoto [b], S. Yajima [b], H. Tsutsui [b], M. Takada [c], A. Maruhashi [a], K. Ono [a]

[a] Research Reactor Institute, Kyoto University, Asashiro-nishi 2-1010, Kumatori-cho, Osaka 590-0494, Japan
[b] Sumitomo Heavy Industries, Osaki 2-1-1, Shinagawa, Tokyo 141-6025, Japan
[c] National Institute of Radiological Sciences, Anagawa 4-9-1, Inage-ku, Chiba-shi 263-8555, Japan

ARTICLE INFO

Keywords:
Cyclotron-based neutron source
Proton cyclotron
Be(p,n) reaction

ABSTRACT

In order to generate epithermal neutrons for boron neutron capture therapy (BNCT), we proposed the method of filtering and moderating fast neutrons, which are emitted from the reaction between a beryllium target and 30 MeV protons accelerated by a cyclotron, using an optimum moderator system composed of iron, lead, aluminum, calcium fluoride, and enriched ^{6}LiF ceramic filter. At present, the epithermal-neutron source is under construction since June 2008 at Kyoto University Research Reactor Institute. This system consists of a cyclotron to supply a proton beam of about 1 mA at 30 MeV, a beam transport system, a beam scanner system for heat reduction on the beryllium target, a target cooling system, a beam shaping assembly, and an irradiation bed for patients.

In this article, an overview of the cyclotron-based neutron source (CBNS) and the properties of the treatment neutron beam optimized by using the MCNPX Monte Carlo code are presented. The distribution of the RBE (relative biological effectiveness) dose in a phantom shows that, assuming a ^{10}B concentration of 13 ppm for normal tissue, this beam could be employed to treat a patient with an irradiation time less than 30 min and a dose less than 12.5 Gy-eq to normal tissue. The CBNS might be an alternative to the reactor-based neutron sources for BNCT treatments.

1. Introduction

At first, the BNCT treatments using KUR (Kyoto University Research Reactor) were adapted for malignant melanoma and brain tumors. The widespread application to the treatment of other diseases such as recurrent head and neck tumors, liver tumors (Suzuki et al., 2007), and mesothelioma (Suzuki et al., 2006) using epithermal neutrons, has resulted in an increased number of clinical trials. In order to obtain good results for deep tumors, a higher dose is required. Moreover, a sufficient neutron yield obtained by using an accelerator-based neutron source that can be located near a hospital would be useful for further developments of BNCT.

Yonai et al. (2003) and Tahara et al. (2006) are already investigating a neutron source using spallation reactions that occur for 30–50 MeV protons incident on a tantalum target. The possibility of exploiting the reaction of several tens of MeV protons incident on a beryllium target, was excluded because of the fast neutrons contamination of the treatment beam. However, a sufficient epithermal neutron yield based on the Be(p,n) reaction could be obtained with an optimum beam-shaping assembly. Our system has the advantage of a larger neutron yield and a lower activation of the target material in comparison with the spallation reactions involving heavy materials.

The neutron transport for optimum treatment beams was simulated by using the Monte Carlo calculation code MCNPX (Pelowitz, 2005). This article reports an overview of the epithermal neutron generator and calculated parameters in phantom.

2. Material and methods

2.1. Cyclotron accelerator and beryllium target

The cyclotron accelerator (HM-30) manufactured by Sumitomo Heavy Industries is employed to provide a ~1 mA, 30 MeV proton beam. In the HM-30 hydrogen negative ions are accelerated and protons up to 30 MeV are derived by charge conversion in a carbon

* Corresponding author.
E-mail address: h-tanaka@rri.kyoto-u.ac.jp (H. Tanaka).

0969-8043/$ - see front matter © 2009 Elsevier Ltd. All rights reserved.
doi:10.1016/j.apradiso.2009.03.096

Table 1
Target material properties for Be, Ta and W.

Target	Melting point (deg)	Boiling point (deg)	Thermal conductivity ($W m^{-1} K^{-1}$)	Neutron yield ($sec^{-1} mA^{-1}$)	Gamma ray yield per one neutron
Be	1278	2970	201	1.90×10^{14}	0.02
Ta	3017	5458	57.5	1.27×10^{14}	0.93
W	3422	5555	174	9.65×10^{13}	1.40

foil stripper. The proton beam derived from HM-30 is led to a beryllium target via a beam transport system. A uniform 120 mm × 120 mm proton beam at the beryllium target is shaped by a controlling magnetic field of two scanning magnets.

Table 1 shows the characteristics of Be, W, and Ta target materials when irradiated by a 1 mA, 30 MeV proton beam. The neutron and gamma ray yields were estimated by using the MCNPX code and the cross-section data of ENDF/B-VII, physical model, and la150 for Be, Ta, and W, respectively. In comparison with the other materials listed in Table 1, Be shows the highest neutron yield, the smallest gamma-ray yield per neutron, the highest thermal conductivity, and a high melting point. A 1 mA, 30 MeV proton beam has a 30 kW power. Such a large heat input needs a target-cooling system. In our system, a Be target is directly cooled by pure compressed water. The compressed water flows through a spiral water channel. 30 MeV protons with a range of 5.8 mm in Be penetrate a 5.5 mm-thick Be target and inject in the compressed cooling water in order to prevent blistering of the target.

With regard to the experimental results for the thermal resistance of a Be target, Tadokoro et al. (2006) indicated that a heat input of 500 W/cm^2 leads to a temperature less than 500 °C. The irradiation area should be expanded to 60 cm^2 for a heat input of 500 W/cm^2 under 30 kW operation. The area of 144 cm^2 scanned by two scanning magnets is sufficient for heat reduction on the target.

In order to evaluate the target activation resulting from 1 year of operation a 2 h irradiation per day with a 1 mA proton current was assumed. The neutron- and proton-induced activation of the three above materials was calculated by using the IRACM code (Tanaka et al., 1997). The nuclei produced in a W target have higher activity and longer half lives than Be and Ta targets. Immediately after the daily operation, the activation rate of a Ta target is four orders of magnitude higher than that of a Be target. The period required for the Ta target until the ambient dose rate becomes 1 mSv h^{-1} is twice of that required for the Be target. Considering the above-mentioned results in terms of neutron yield, thermal properties, and activation level, the Be target was chosen.

2.2. Beam-shaping assembly (BSA)

Yanch et al. (1991) found out that for BNCT treatments at a 10 cm depth in the head, the most effective neutron energy is 10 keV and the most effective neutron energy range is between 4 eV and 40 keV.

In the reaction between 30 MeV protons and a Be target, the neutrons that are emitted in the forward direction have an energy of up to 28 MeV. In order to reduce the neutron energy to the epithermal energy range, a BSA composed of a moderator and a shaper has been employed. The moderator is used to reduce the energy from the maximum value of 28 MeV with low capture cross-section. The shaper is used to obtain the 10 keV optimum energy mentioned above.

Fig. 1 shows the schematic layout of the BSA. The moderator materials are Pb and Fe. The Pb component, used as a breeder and a reflector for high energy neutrons, was installed near the target.

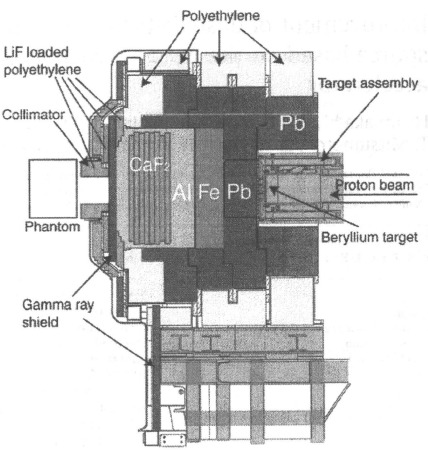

Fig. 1. Schematic layout of the BSA to obtain an epithermal neutron beam using a 30 MeV proton beam incident on a beryllium target.

The Fe component, mainly used as a moderator, was installed after the Pb component. With regard to the shaper, AlF_3 is often used in the design of an epithermal neutron generator (Liu et al., 2004; Culbertson et al., 2004) and the material density should be high in order to form a compact BSA. It is difficult to increase the AlF_3 density because it sublimes at a temperature of 1040 °C under atmospheric pressure. Therefore, we focused on Al and CaF_2 instead of AlF_3.

The optimum thickness of each component was determined through the calculation of the dose distribution in the phantom composed of soft average tissue of an adult male (ICRU-44) by using the MCNPX code.

In order to prevent the exposure of the patient to the fast-neutron radiation, the moderator, the shaper, and the front surface of the collimator are surrounded by polyethylene blocks.

Furthermore, in order to accurately set the patient in the position determined by the treatment planning system, an X-ray tube and an imaging plate are installed. The pair of X-ray tube and imaging plate can be moved to the neutron beam side and an image of the "beam's eye view" can be obtained. Laser markers are also installed; the irradiation position is set by a marking on the skin.

3. Results and discussion

All the following results are related to a 1 mA, 30 MeV proton beam.

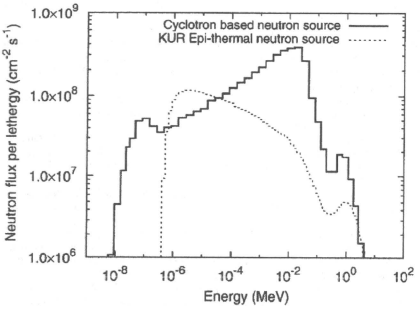

Fig. 2. Comparison between the CBNS neutron spectrum and the KUR one.

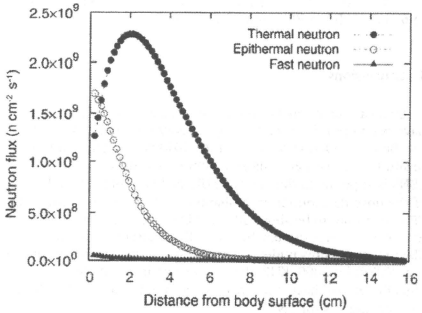

Fig. 3. Neutron flux components (thermal, epithermal and fast) in phantom.

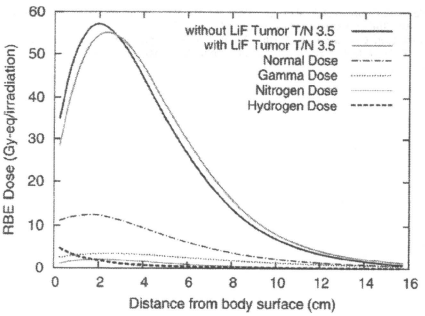

Fig. 4. RBE dose components in phantom.

3.1. Free beam properties

Fig. 2 shows the CBNS neutron flux spectrum under the free-air condition evaluated at the surface of the gamma-ray shield in comparison with the KUR one, which is most-often used in the BNCT treatments (Sakurai and Kobayashi, 2000). The CBNS neutron spectrum has a peak in the 10–20 keV energy range.

In some of the BNCT literature, the epithermal range is defined as the interval from 0.5 eV to 10 keV, which is recommended by IAEA-TECDOC1223 (2001). However, we designed the moderator to fulfill the maximization of epithermal neutron flux with the interval from 4 eV to 40 keV, which is more effective to treat deep tumors. Furthermore, Blue et. al. (1993) showed the calculated RBE value as a function of neutron energy and found out that the RBE of the energy of 40 keV was less than 3.0. They also showed the RBE of the energy of around 0.5 eV was less than 3.0. It is appropriate to define the value of 40 keV as boundary energy between epithermal and fast neutron. Consequently, in this article, the definition of the epithermal energy range is from 0.5 eV to 40 keV. The energy region below 0.5 eV is defined as the thermal region; that above 40 keV, as the fast-neutron region.

The fast-neutron and gamma-ray dose contaminations per epithermal neutron for CBNS under the free-air condition are 5.84×10^{-13} and 7.75×10^{-14} Gy cm^2, respectively. Each absorbed dose value was obtained by using the neutron flux at the gamma-ray shield and the flux-to-dose conversion factors published in ICRP-74. The human tissue components were assumed to be H: 11.1, C: 12.6, N: 2.0, and O: 74.3 (wt%). The fast-neutron and gamma-ray dose contaminations per epithermal neutron for KUR under the free-air condition are 9.10×10^{-13} and 2.40×10^{-13} Gy cm^2, respectively (Sakurai and Kobayashi, 2000). With regard to the fast neutrons and gamma rays contaminations the CBNS facility is superior to KUR one.

3.2. Beam characteristics in phantom

Fig. 3 shows the evaluation of the CBNS neutron flux components in a phantom located in front of the collimator. The diameter of the collimator aperture and phantom are 16 and 26 cm, respectively. The maximum value of thermal neutron flux is 2.3×10^9 cm^{-2} s^{-1} at a depth of 2.3 cm in phantom.

The prescribed dose is determined by the differential boron accumulation in tumor and normal cells (T/N ratio) and the boron concentration in the blood of the patient. The RBEs assumed for nitrogen, hydrogen, and gamma rays are 3.0, 3.0, and 1.0, respectively. The compound biological effectiveness (CBE) factors for tumor and normal brain are 3.8 and 1.35, respectively. The T/N ratio of 3.5 is employed. The boron concentration is assumed to be 13 ppm. The therapeutic time is determined by the dose limit for the normal brain of 12.5 Gy-eq. Fig. 4 shows the distribution of the RBE dose components in the phantom. Under the above hypotheses, the RBE dose in tumor reaches a maximum value of 57 Gy-eq at a depth of about 2.3 cm in phantom and the irradiation time is less than 30 min. The sufficient dose for killing the tumor is at least 30 Gy-eq. The CBNS facility can treat a tumor located within a depth of 5.5 cm, with the RBE dose of 30 Gy-eq by single irradiation. With regard to the irradiation of deeper tumors, the bilateral irradiation can be adopted to raise the prescribed dose. At a depth of 8 cm, the RBE dose is about 15 Gy-eq. Therefore CBNS can treat tumors situated at almost all the positions in the brain by using the bilateral irradiation.

Furthermore, to improve the dose distribution at a deeper position, an enriched ^{6}LiF ceramic filter (thickness of 6 mm) placed after the gamma ray shield can be used. The enriched ^{6}LiF filter produces a more ideal neutron spectrum because of filtering in the low energy region. The thickness of ^{6}LiF filter is optimized to fulfill a therapeutic time of less than 60 min. Fig. 4 shows the dose distribution in phantom using the enriched ^{6}LiF ceramic

filter. The use of this filter increases the treatable depth from 5.5 to 6.0 cm with the RBE dose of 30 Gy-eq.

4. Conclusions

By means of Monte Carlo simulations a moderator and a shaper have been optimized for the high energy neutrons emitted from the Be(p,n) reaction with a 1 mA, 30 MeV proton beam. With regard to the fast neutrons and gamma rays dose contamination, CBNS is superior to the current KUR facility. From the evaluation of the dose distribution in a phantom the irradiation time using CBNS turns out to be about 30 min. CBNS becomes a powerful tool for treating deep tumors by using the bilateral irradiation. The CBNS facility is now under construction and the aim is to establish it at KURRI by 2009. KUR also will restart in the middle of 2009. Thus KURRI will have both the reactor- and the accelerator-based neutron sources for BNCT.

References

Blue, T.E., Gupta, N., Woollard, J.E., 1993. A calculation of the energy dependence of the RBE of neutrons. Phys. Med. Biol. 38, 1693–1712.

Culbertson, C.N., Green, S., Mason, A.J., Picton, D., Baugh, G., Hugtenburg, R.P., Yin, Z., Scott, M.C., Nelson, J.M., 2004. In-phantom characterisation studies at the Birmingham accelerator-generated epithermal neutron source (BAGINS) BNCT facility. Appl. Radiat. Isot. 61, 733–738.

IAEA TECDOC 1223, 2001. Current status of neutron capture therapy.

Liu, Y.W.H., Huang, T.T., Jiang, S.H., Liu, H.M., 2004. Renovation of epithermal neutron beam for BNCT at THOR. Appl. Radiat. Isot. 61, 1039–1043.

Pelowitz, D.B., 2005. MCNPX user's manual—version 2.5.0. Los Alamos National Laboratory Report LA-CP-05-0369.

Sakurai, Y., Kobayashi, T., 2000. Characteristics of the KUR heavy water neutron irradiation facility as a neutron irradiation field with variable energy spectra. Nucl. Instrum. Methods A 453, 569–596.

Suzuki, M., Sakurai, Y., Masunaga, S., Kinashi, Y., Nagata, K., Maruhashi, A., Ono, K., 2006. Feasibility of boron neutron capture therapy (BNCT) for malignant pleural mesothelioma from a viewpoint of dose distribution analysis. Int. J. Radiat. Oncol. Biol. Phys. 66 (5), 1584–1589.

Suzuki, M., Sakurai, Y., Hagiwara, S., Masunaga, S., Kinashi, Y., Nagata, K., Maruhashi, A., Ono, K., 2007. First attempt of boron neutron capture therapy (BNCT) for hepatocellular carcinoma. Jpn. J. Clin. Oncol. 37 (5), 376–381.

Tadokoro, T., Kawakubo, Y., Seki, H., Tayama, R., Umegaki, K., Baba, M., Kobayashi, T., 2006. Feasibility study on a common use accelerator system of neutron production for BNCT and radionuclide production for PET. Advances in neutron capture therapy 2006. In: Proceedings of ICNCT-12, pp. 304–307.

Tahara, Y., Oda, Y., Shiraki, T., Tsutsui, T., Yokobori, H., Yonai, S., Baba, M., Nakamura, T., 2006. Engineering design of a spallation reaction-based neutron generator for boron neutron capture therapy. J. Nucl. Sci. Technol. 43 (1), 9–19.

Tanaka, S., Fukuda, M., Nishimura, K., 1997. A code system to calculate induced radioactivity produced by ions and neutrons. JAERI-Data/Code 97–019.

Yanch, J.C., Zhou, X.L., Brownell, G.L., 1991. A Monte Carlo investigation of the dosimetric properties of monoenergetic neutron beams for neutron capture therapy. Radiat. Res. 126, 1–20.

Yonai, S., Aoki, T., Nakamura, T., Yashima, H., Baba, M., Yokobori, H., Tahara, Y., 2003. Feasibility study on epithermal neutron field for cyclotron-based boron neutron capture therapy. Med. Phys. 30 (8), 2021–2030.

Applied Radiation and Isotopes 67 (2009) S325–S327

Contents lists available at ScienceDirect

Applied Radiation and Isotopes

journal homepage: www.elsevier.com/locate/apradiso

Bystander effect-induced mutagenicity in HPRT locus of CHO cells following BNCT neutron irradiation: Characteristics of point mutations by sequence analysis

Yuko Kinashi *, Minoru Suzuki, Shinichiro Masunaga, Koji Ono

Research Reactor Institute, Kyoto University, Kumatori-cho, Sennan-gun, Osaka, Japan

ARTICLE INFO

Keywords:
Alpha particle
Neutron
BSH
HPRT
Point mutation

ABSTRACT

To investigate bystander mutagenic effects induced by alpha particles during boron neutron capture therapy (BNCT), we mixed cells that were electroporated with borocaptate sodium (BSH), which led to the accumulation of ^{10}B inside the cells, with cells that did not contain the boron compound. BSH-containing cells were irradiated with α particles produced by the $^{10}B(n,\alpha)^7Li$ reaction, whereas cells without boron were only affected by the $^1H(n,\gamma)^2H$ and $^{14}N(n,p)^{14}C$ reactions.

The frequency of mutations induced in the hypoxanthine-guanine phosphoribosyltransferase (HPRT) locus was examined in Chinese hamster ovary (CHO) cells irradiated with neutrons (Kyoto University Research Reactor: 5 MW). Neutron irradiation of 1:1 mixtures of cells with and without BSH resulted in a survival fraction of 0.1, and the cells that did not contain BSH made up 99.4% of the surviving cell population. Using multiplex polymerase chain reactions (PCRs), molecular structural analysis indicated that most of the mutations induced by the bystander effect were point mutations and that the frequencies of total and partial deletions induced by the bystander effect were lower than those resulting from the α particles produced by the $^{10}B(n,\alpha)^7Li$ reaction or the neutron beam from the $^1H(n,\gamma)^2H$ and $^{14}N(n,p)^{14}C$ reactions.

The types of point mutations induced by the BNCT bystander effect were analyzed by cloning and sequencing methods. These mutations were comprised of 65.5% base substitutions, 27.5% deletions, and 7.0% insertions. Sequence analysis of base substitutions showed that transversions and transitions occurred in 64.7% and 35.3% of cases, respectively. G:C→T:A transversion induced by 8-oxo-guanine in DNA occurred in 5.9% of base substitution mutants in the BNCT bystander group. The characteristic mutations seen in this group, induced by BNCT α particles, differed from those typical of gamma ray radiation.

1. Introduction

We previously described the mutagenicity of thermal neutrons in Chinese hamster ovary (CHO) cells and presented evidence for the increase of this mutagenicity in the presence of boron (Kinashi et al., 1997, 2000). In boron neutron capture therapy (BNCT) experiments, boron was located both inside and outside the cells. Clinically, one problem associated with BNCT is the potential mutagenic effect of the therapy on normal cells that do not take up the boron compounds, but are located near the boron-containing tumor cells. In this study, we investigated the mutagenic effects of this therapy on cells that did not contain boron (no-boron cells), but were located near cells that contained ^{10}B following electroporation with borocaptate sodium (BSH) (BSH-electroporated cells).

Mutations induced by the bystander effect following BNCT neutron radiation were assessed via evaluation of the c-DNA of nine exons located in the hypoxanthine-guanine phosphoribosyltransferase (HPRT) locus.

2. Materials and methods

2.1. Cell culture and electroporation

CHO K-1 (wild-type) cells were cultured at 37 °C in a humidified 5% CO_2 atmosphere in Eagle's α-minimal essential medium (MEM). CHO cells exponentially growing in MEM were trypsinized and cell suspensions containing 10 ppm BSH were placed into the chamber (maximum effective volume of 0.8 ml) of a Gene Pulser system for electroporation (Bio-Rad Laboratories). After electroporation the cells were washed twice with PBS, the medium was replaced with MEM without the boron-containing

* Corresponding author. Tel.: +81 72 451 2437; fax: +81 72 451 2627.
E-mail address: kinashi@rri.kyoto-u.ac.jp (Y. Kinashi).

0969-8043/$ - see front matter © 2009 Elsevier Ltd. All rights reserved.
doi:10.1016/j.apradiso.2009.03.072

compound, and the viable cells were counted. The no-boron cells were also trypsinized and counted, and the BSH-electroporated cells were placed in a flask containing no-boron CHO cells at a cellular ratio of 1:1. After confirming that the cells were attached to the flask, the cells were irradiated at room temperature with neutrons from a reactor at Kyoto University. The total absorbed dose resulting from thermal or epithermal neutron irradiation was calculated by the sum of the absorbed doses. The details of this calculation method were described previously (Kobayashi and Kanda, 1982; Kitao, 1975).

2.2. HPRT mutation assays

To determine the mutant frequencies, each irradiated culture containing at least 10^6 cells was incubated in a non-selective medium for 7–9 days to allow phenotype expression. Then, 2×10^5 cells were added to each of twenty 100 mm plastic dishes containing 5 μg/ml 6-thioguanine, incubated for 10 days, and the mutant colonies were counted. The mutant frequencies are expressed as the number of resistant colonies divided by the total number of viable cells, which was determined using the cloning efficiency at the time of selection.

2.3. Analysis of the molecular structure of the HPRT mutations and the types of point mutations using direct sequencing of PCR fragments

In the mutation analysis, neutron irradiation at the applied fluence resulted in a cellular survival fraction of 0.1. At this fluence, the survival fractions of the no-boron cells and the BSH-electroporated cells were 0.7 and 0.004, respectively (Table 1). The cell population of the samples after neutron irradiation comprised 99.4% no-boron cells and 0.6% BSH-electroporated cells. The DNA extraction procedure has been described in detail previously (Kinashi et al., 1995). Structural analysis of the HPRT gene was carried out using a modified multiplex polymerase chain reaction (PCR) amplification technique. Three sets of PCRs were carried out to amplify exons 2, 3, 7/8, and 9; exons 4, 5, and 6; and exon 1. The molecular structure of the HPRT genes were divided into three categories: no change (normal-size exons 1 through 9 were present), partial deletion(s) (the absence of between one and eight of the exons as revealed by PCR analysis), and total deletion (all nine HPRT exons were missing).

2.4. Statistical analysis

Statistical significance was calculated using Student's t tests. Results were considered significant for values of $p<0.05$.

3. Results and discussion

Fig. 1 shows the patterns of HPRT mutations. The molecular nature of the point mutations was analyzed using the direct PCR fragment sequences of exons 1 and 9. In this experiment, fewer partial and total deletions in the HPRT gene were observed in the cells mixed with BSH-electroporated cells than in cells directly irradiated by the α particles that resulted from the $^{10}B(n,\alpha)^7Li$ reaction. Due to the bystander effect, mutations were supposed to be induced in the cells located near the BSH-containing cells. These mutants were not irradiated directly by α particles. Molecular structural analysis indicated that most of the mutations induced by the bystander effect (the 4th bar in the figure) were point mutations and that the frequencies of total and partial deletions induced by the bystander effect were lower than those induced by other forms of neutron irradiation (the 1st to 3rd bars in the figure). The 1st bar of Fig. 1 shows the mutations induced by the $^1H(n,\gamma)^2H$ and $^{14}N(n,p)^{14}C$ reactions. The 2nd and 3rd bars show the mutations caused by α particles produced by the $^{10}B(n,\alpha)^7Li$ reaction. The 2nd bar represents cells containing BSH, while the 3rd signifies cells characterized by both intra- and extracellular boron. The mutation frequencies in the 2nd and 3rd cell groups were different, but the mutation pattern was similar in that numerous deletions were contained.

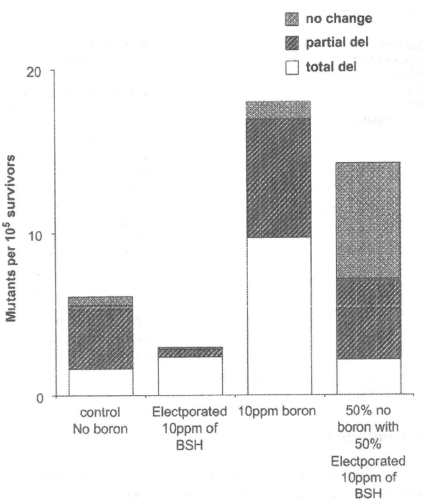

Fig. 1. The patterns of HPRT mutations. Total deletion indicates absence of all nine HPRT exons. Partial deletion indicates absence of between one and eight exons. No change means point mutation that normal-size exons one through nine were present.

Table 1
Survival fraction and mutant frequency following neutron irradiation at the fluence of $1.4 \times 10^{11}/cm^{2a}$

Treatment	Radiation dose (Gy)	Survival fraction	Mutants per 10^5 cells[b]
No-boron	0.6	0.7 ± 0.05	1.5 ± 0.5
Electroporation with 10 ppm BSH	3.9	0.004 ± 0.001	3.0 ± 1.0
Bystander α particle irradiation	2.2	0.1 ± 0.02	10.0 ± 4.0

[a] This neutron fluence resulted in a survival fraction of 0.1 following neutron irradiation of samples with a 1:1 ratio of no-boron cells to cells electroporated in the presence of 10 ppm BSH.
[b] Mean of the mutation frequency ± SE from three or more experiments.

Table 2
Types of point mutations induced by BNCT bystander effect and by γ-ray irradiation.

Types	BNCT bystander (%)	γ-ray irradiation (%)
Base substitution	65.5	62
Deletions	27.5	30
Insertions	7	8

Table 3
Patterns of base substitutions induced by BNCT bystander effect and by γ-ray irradiation.

	BNCT bystander	γ-ray irradiation
Transition		
G:C→A:T	4	6
A:T→G:C	8	1
Total	12	7
(%)	35.3	31.8
Transversion		
G:C→T:A	2	10
G:C→C:G	5	4
A:T→C:G	0	1
A:T→T:A	15	0
Total	22	15
(%)	64.7	68.2

In a previous study, we reported that neutron irradiation induced partial and total deletion mutations at high frequencies. In particular, the partial and total deletions were more commonly found after neutron irradiation than gamma irradiation (Kinashi et al., 2000). In this study, we analyzed the induced mutations and observed that point mutations were more frequently induced in bystander cells than in cells irradiated with α particles produced by the $^{10}B(n,\alpha)^{7}Li$ reaction or with neutrons generated by the $^{1}H(n,\gamma)^{2}H$ and $^{14}N(n,\rho)^{14}C$ reactions.

A previous study that examined the bystander effect caused by α particles reported that most of the mutations identified in the bystander cells were point mutations (Huo et al., 2001). Our results agree with those findings and suggest that the mutations seen in bystander cells result from a mechanism distinct from that of direct neutron beam irradiation in BNCT.

Tables 2 and 3 illustrate the mutation types and various base substitutions induced by the bystander effect of BNCT. The cloning and sequencing analysis showed that 65.5% of point mutations were base substitutions, 27.3% were deletions, and 7.0% were insertions. The characteristics of mutations induced by the BNCT-bystander effect were similar to those that typically result from gamma ray induced mutagenesis (Grosovsky et al., 1988; Nohmi and Masumura, 2005).

Base substitutions induced by ionizing radiation are marked by a predominance of G:C→T:A transversions. This mutation is induced by 8-oxo-guanine in DNA (Kasai et al., 1993). Clinically, it has been noticed that in lung cancer the p53 oncogene displays G:C→T:A transversion (Iggo et al., 1990). This evidence suggests that G:C→T:A transversion may be related to radiation-induced carcinogenesis. Our results showed that G:C→T:A transversion in bystander cells was uncommon, occurring in only 5.9% base substitution mutants. The G:C→T:A transversion in radiation-induced point mutations is caused by radiation-induced strand breakage (Grosovsky et al., 1988). Our results therefore suggest that the mutations caused by the bystander effect in BNCT were not attributable to radiation-induced strand breaks and that the bystander mutations were caused by mechanisms other than direct irradiation.

Acknowledgments

This study was supported by a Grant-in-Aid for Scientific Research from the Ministry of Education, Culture, Sports, Science and Technology of Japan.

References

Grosovsky, A.J., DE Boer, J.G., DE Jong, P.J., Drobetsky, E.A., Glickman, B.W., 1988. Base substitutions, frameshifts, and small deletions constitute ionizing radiation-induced point mutations in mammalian cells. Proc. Nat. Acad. Sci. USA 85, 185–188.

Huo, L., Nagasawa, H., Little, J.B., 2001. HPRT mutants induced in bystander cells by very low fluencies of alpha particles result primarily from point mutations. Radiat. Res. 156, 521–525.

Iggo, R., Gatter, K., Bartek, J., Lane, D., Harris, A.L., 1990. Increased expression of mutant forms of p53 oncogene in primary lung cancer. Lancet 335, 675–679.

Kasai, H., Chung, M.H., Yamamoto, F., Ohtsuka, F., Laval, J., Grooiman, A.P., Nishimura, S., 1993. Formation, inhibition of formation, and repair of oxidative 8-hydroxyguanine DNA damage. Basic Life Sci. 61, 257–262.

Kinashi, Y., Nagasawa, H., Little, J.B., 1995. Molecular structure analysis of 417 HPRT mutations induced by restriction endonucleases in Chinese hamster ovary (CHO) cells. Mutat. Res. 326, 83–92.

Kinashi, Y., Masunaga, S., Takagaki, M., Ono, K., 1997. Mutagenic effect at HPRT locus induced in Chinese hamster ovary cells by thermal neutrons with or without boron compound. Mutat. Res. 377, 211–215.

Kinashi, Y., Sakurai, Y., Masunaga, S., Suzuki, M., Takagaki, M., Akaboshi, M., Ono, K., 2000. Molecular structure analysis of HPRT mutations induced by thermal and epithermal neutrons in Chinese hamster ovary cells. Radiat. Res. 154, 313–318.

Kitao, K., 1975. A method for calculating the absorbed dose near-interface from $^{10}B(n,\alpha)^{7}Li$ reaction. Radiat. Res. 61, 204–315.

Kobayashi, T., Kanda, K., 1982. Analytical calculation of boron-10 dosage in cell nucleus for neutron capture therapy. Radiat. Res. 91, 77–94.

Nohmi, T., Masumura, K., 2005. Molecular nature of intra chromosomal deletions and base substitutions by environmental mutagens. Environ. Mol. Mutagenesis 45, 150–161.

Nuclear Instruments and Methods in Physics Research B 267 (2009) 1970–1977

Contents lists available at ScienceDirect

Nuclear Instruments and Methods in Physics Research B

journal homepage: www.elsevier.com/locate/nimb

Characteristics comparison between a cyclotron-based neutron source and KUR-HWNIF for boron neutron capture therapy

H. Tanaka [a,*], Y. Sakurai [a], M. Suzuki [a], S. Masunaga [a], Y. Kinashi [a], G. Kashino [a], Y. Liu [a], T. Mitsumoto [b], S. Yajima [b], H. Tsutsui [b], A. Maruhashi [a], K. Ono [a]

[a] Research Reactor Institute, Kyoto University, Asashiro-nishi 2-1010, Kumatori-cho, Osaka 590-0494, Japan
[b] Sumitomo Heavy Industries, Osaki 2-1-1, Shinagawa, Tokyo 141-6025, Japan

ARTICLE INFO

Article history:
Received 22 July 2008
Received in revised form 15 January 2009
Available online 27 March 2009

PACS:
87.56.–v
87.56.Bd
87.55.Gh
87.55.Dk

Keywords:
Accelerator-based neutron source
Boron neutron capture therapy
Proton cyclotron
Be(p,n) reaction

ABSTRACT

At Kyoto University Research Reactor Institute (KURRI), 275 clinical trials of boron neutron capture therapy (BNCT) have been performed as of March 2006, and the effectiveness of BNCT has been revealed. In order to further develop BNCT, it is desirable to supply accelerator-based epithermal-neutron sources that can be installed near the hospital. We proposed the method of filtering and moderating fast neutrons, which are emitted from the reaction between a beryllium target and 30-MeV protons accelerated by a cyclotron accelerator, using an optimum moderator system composed of iron, lead, aluminum and calcium fluoride. At present, an epithermal-neutron source is under construction from June 2008. This system consists of a cyclotron accelerator, beam transport system, neutron-yielding target, filter, moderator and irradiation bed.

In this article, an overview of this system and the properties of the treatment neutron beam optimized by the MCNPX Monte Carlo neutron transport code are presented. The distribution of biological effect weighted dose in a head phantom compared with that of Kyoto University Research Reactor (KUR) is shown. It is confirmed that for the accelerator, the biological effect weighted dose for a deeply situated tumor in the phantom is 18% larger than that for KUR, when the limit dose of the normal brain is 10 Gy-eq. The therapeutic time of the cyclotron-based neutron sources are nearly one-quarter of that of KUR. The cyclotron-based epithermal-neutron source is a promising alternative to reactor-based neutron sources for treatments by BNCT.

1. Introduction

Boron neutron capture therapy (BNCT) is a modality to kill a cancer cell by an α particle and a Li nucleus emitted from the capture reaction between a thermal neutron and a ^{10}B atom added in the medicine that easily accumulates in a cancer cell. The emitted α particle and Li nucleus have short ranges of 9 μm and 5 μm, respectively, and total range is 14 μm corresponding to the cell size. As a result, their energy is mostly deposited within a cell. Therefore, BNCT is a unique modality that has higher cell selectivity than other radiotherapies.

At first, the BNCT treatments using Kyoto University Research Reactor (KUR) were adapted for malignant melanoma and brain tumors. Heavy-water neutron irradiation facility (HWNIF) of KUR was upgraded in March 1996. Its wide application to the treatment of the other disease such as recurrent head and neck tumors, liver tumors [1], and mesothelioma [2] using epithermal-neutrons has resulted in an increase in the number of trial cases. Seventy percent of the cases were treated after December 2001. In order to obtain good treatment results for a deeply situated body tumor, a higher dose is required.

KUR has been stopping the operation since March 2006 because of the return of high-enriched uranium fuels. However, we have a plan to install low-enriched uranium fuels to operate KUR for one decade. More clinical trials will be carried out to show the effectiveness of BNCT. Moreover, a sufficient neutron yield obtained by using an accelerator-based neutron source that can be located near a hospital is required for the further development of BNCT.

Some groups are already investigating a neutron source using spallation reactions between several tens of MeV protons and heavy materials such as lead, tungsten and tantalum [3,4]. As for the combination of several tens of MeV protons and a beryllium target, the examination was excluded because of the contamination of the treatment beam (epithermal-neutron beam) by fast neutrons. However, we confirmed that a sufficient epithermal-neutron yield based on the Be(p,n) reaction could be obtained with an optimum beam-shaping assembly. Our system has the advantage of lower

* Corresponding author. Tel.: +81 72 451 2468; fax: +81 72 451 2620.
E-mail address: h-tanaka@rri.kyoto-u.ac.jp (H. Tanaka).

0168-583X/$ - see front matter © 2009 Elsevier B.V. All rights reserved.
doi:10.1016/j.nimb.2009.03.095

activity and larger neutron yield of targets as compared with the spallation reactions involving heavy materials.

Our system consists of a cyclotron accelerator promising a proton beam of ~1 mA at 30 MeV, a beam transport system, a beam scanner system for heat reduction on the beryllium target, a target-cooling system, a beam-shaping assembly, a multi-leaf collimator and an irradiation bed for patients in both sitting and decubitus positions. We simulated the neutronics for optimum treatment beams using the Monte Carlo calculation code MCNPX [5]. In this article, we report the system of our epithermal-neutron generator and the simulated characteristics compared with that of KUR.

2. Materials and methods

2.1. Cyclotron-based neutron source (CBNS)

2.1.1. Accelerator and beam transport

Fig. 1 shows schematic layout of a cyclotron-based neutron source in Innovation Research Laboratory Medical Area at KURRI. We employ the cyclotron accelerator (HM-30) manufactured by Sumitomo Heavy Industries (SHI) to promise ~1 mA at 30 MeV proton beam. SHI has the technology to manufacture various types of cyclotron accelerators for the production of radioactive medicines for positron emission tomography (PET). Accelerating particles of HM-30 are hydrogen negative ions, and the particles accelerated up to 30 MeV are derived by the charge conversion in a carbon foil stripper. HM-30 dimensions of 3030-mm width × 1620-mm length × 1724-mm height. A proton beam derived from HM-30 is led to the beryllium target via a beam transport system. Two electromagnetic scanning coils are inserted at the end of the beam transport system for beam spread in order to reduce the heat produced in the Be target. A uniform proton beam with a square shape of 120 mm × 120 mm is formed by controlling magnetic field of each scanning magnet. The principle of scanning

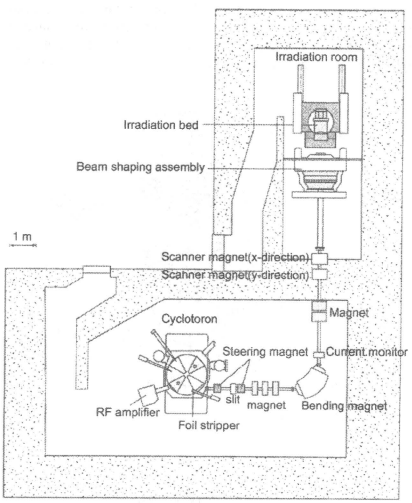

Fig. 1. Schematic layout of cyclotron-based neutron source.

is to use the difference of the scanning frequencies between the X- and Y-axes magnets excited by triangle waves.

2.1.2. Beryllium target

In order to select a suitable target material, it is important to consider the characteristics such as neutron yield, neutron energy, thermal properties and the activation on proton irradiation in terms of the maintenance of a target. Table 1 shows the characteristics of Li, Be, W and Ta as target materials when irradiated by a 1-mA, 30-MeV proton beam. The neutron and gamma-ray yields were estimated by MCNPX and the cross-section data. The target thickness is more than the range of protons at 30 MeV in each of the target materials. In order to calculate the neutron yield of the Ta target, the LAHET code [6] with a physics model was used because the evaluated nuclear-cross-section data of La150 do not contain Ta data.

Among the materials listed in Table 1, Be has the highest neutron yield and the smallest gamma-ray yield per neutron. The neutron yield is high in the order of Ta, W and Li. Because of the low melting point of Li, it is difficult to maintain a Li target stable under 1-mA, 30-MeV proton beam irradiation.

Further, In Table 1, Be has the highest thermal conductivity and a high melting point. A 1-mA, 30-MeV proton beam has a power of 30 kW; this implies a heat input of 30 kW to the target irradiated using this beam. Such a large heat input necessitates a target-cooling system. In our system, a Be target is directly cooled by pure compressed water. The compressed water flows through a spiral graphite water channel; the graphite is prevented from activation. Protons (30-MeV) with a range of 5.8 mm in Be penetrate a 5.5-mm-thick Be target and inject in the compressed cooling water in order to prevent blistering of the target. Most of the low-energy protons with an energy of less than 2 MeV cannot produce neutrons while passing through Be because the threshold energy of reaction between proton and Be is ~2 MeV.

With regard to the experimental results for the thermal resistance of a Be target, Tadokoro et al. indicated that a heat input of 500 W/cm^2 leads to a temperature of less than 500 °C [7]. The irradiation area should be expanded to 144 cm^2 for a heat input of 200 W/cm^2 under 30-kW operation.

The activation of a target should be as low as possible in order to avoid additional expenses that are otherwise incurred by remote handling devices and heavy radiation shielding. Low activation is also important for hospital management with regard to the maintenance, storage and control of targets.

For evaluating target activation resulting from one year of operation we assumed 2-h irradiation per day with a proton current of 1 mA. Fig. 2 shows the relationship between the ambient dose equivalent at 1 cm and the elapsed time after one year of operation. Induced radioactivity analysis code (IRAC) can calculate the neutron- and proton-induced activation of target material [8]. The nuclei produced in a W target have higher activity and longer half lives than Be and Ta targets. Immediately after one year of operation, the activation rate of a Ta target is four order of magnitude higher than that of a Be target. The period required by the Ta target until the ambient dose rate becomes 1 mSv/h, is twice of that required by the Be target. Considering the above-mentioned results in terms of the neutron yield, thermal properties, and activation level, we selected the Be target.

2.1.3. Beam-shaping assembly

Yanch et al. revealed that for BNCT treatments at a 10-cm depth of the head, 10 keV is the most effective neutron energy and 4 eV to 40 keV is the most effective energy range [9]. In terms of the design of an accelerator-based moderator, it is necessary to form the neutron irradiation field with an energy spectrum peaking at around 10 keV. In the reaction between 30-MeV protons and a Be target,

Table 1
Target material property compared with Li, Be, Ta and W.

Target	Melting point (°C)	Boiling point (°C)	Thermal conductivity (W/m/K)	Neutron yield (/s/mA)	Gamma-ray yield (s/mA)	Gamma-ray yield per one neutron	Cross-section data
Li	180	1340	84.7	1.14E+14	9.80E+12	0.09	ENDF-VII
Be	1278	2970	201	1.90E+14	3.35E+12	0.02	ENDF-VII
Ta	3017	5458	57.5	1.27E+14	1.18E+14	0.93	Physics model
W	3422	5555	174	9.65E+13	1.35E+14	1.40	la150

the neutrons that are emitted forward direction have an energy of up to 28 MeV. Therefore, in order to treat a deep tumor, it is necessary to reduce the neutron energy to the range of epithermal energy. For this purpose, our system has two components: a moderator and a shaper. The moderator is used to reduce the energy from the maximum value of 28 MeV with low capture cross-section. The shaper is used to obtain the optimum energy such as 10 keV mentioned above.

Fig. 3 shows the schematic layout of the moderator, shaper, (called beam-shaping assembly: BSA) and irradiation room. The moderator materials are Pb and Fe. Pb has a cross-section of ~1 barn for the (n,2n) reaction with the maximum neutron energy of larger than 10 MeV. Further, Pb has the inelastic scattering cross-section of ~1 barn for the incident neutron energy of larger than 1 MeV. Fe has a smaller cross-section for the (n,2n) reaction than Pb has, but the inelastic scattering cross-section of Fe is larger than that of Pb at an incident neutron energy of several MeV. Therefore, a Pb component was installed near the target region and a Fe component was installed after the Pb component. The Pb component was placed around the Be target assembly as a reflector in order to reflect the neutrons that were back-scattered by the Be target. The target assembly is removable in order to facilitate target replacement.

The shaper is made of Al and CaF_2 and serves to reduce the neutron energy to the epithermal energy region. The total neutron cross-section of Al exhibits valleys at incident neutron energies of around 27 and 70 keV. This implies that the neutrons with these energies have a small probability of reacting with Al. Further, although 70-keV neutrons raise the normal dose, F has the resonance cross-section at a neutron energy of larger than several tens keV. Consequently, the combination of Al and F limits the neutron energy to around 27 keV.

The combination of 69% AlF_3, 30% Al and 1% ^{6}LiF (called FLUENTAL™ developed by VTT Corporation at Finland) is often used in the design of an epithermal-neutron generator [10]. In order to obtain intense neutron flux, the moderator and shaper size should be small with sufficient ability for moderating and shaping. It is recommended that the material density of the shaper should be high.

FLUENTAL™ is supplied as powder; it is difficult to increase its density because AlF_3 sublimes at a temperature of 1040 °C under atmospheric pressure. Therefore, we focus our attention on CaF_2 that is easily available on a commercial basis. CaF_2 dose not have good mechanical strength; therefore, it was formed in a disk shape and placed in an Al container.

Epithermal neutrons are passed through the moderator and shaper and led to a collimator that is placed after a gamma shield made of Pb. The collimator is composed of ^{nat}LiF-loaded polyethylene blocks having a thickness of 1.5 cm. The collimator aperture can be adjusted up to ϕ25 cm and formed to any shape in order to fit the irradiation field. Patients can easily seat to insert the foot in the cone shape of the collimator.

Fig. 4 shows the calculation results of energy reduction process in the moderator and shaper. After the neutrons have passed through the moderator, which is composed of Pb and Fe, their energy spectrum exhibits a peak at 1 MeV. This implies that the moderator can effectively reduce the energy that is higher than 1 MeV. After coming out of the moderator, these neutrons pass through the shaper, which is composed of Al and CaF_2, that further reduces their energy from 1 MeV to the epithermal-neutron region of 10–20 keV. The optimum thickness of each component was determined by the Monte Carlo simulation using the property of the distribution of biological effect weighted dose in a phantom.

In order to prevent the exposure of a patient to fast-neutron radiation, the moderator and shaper (particularly the front surface of the collimator) are surrounded by polyethylene blocks. These polyethylene blocks also serve as a shield around the irradiation room.

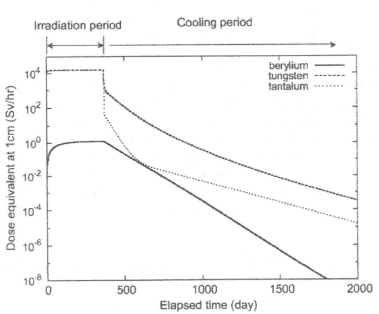

Fig. 2. Relationship between the elapsed time after one-year irradiation operation and the activation of Be, W and Ta targets.

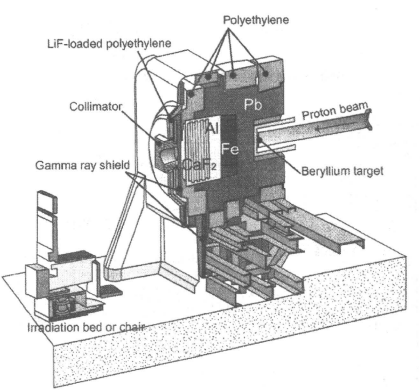

Fig. 3. Schematic layout of a beam-shaping assembly for epithermal neutron generator using 30-MeV proton cyclotron and Be target.

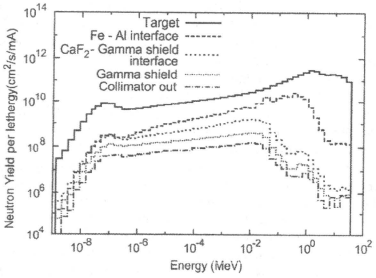

Fig. 4. Neutron energy spectrum at each evaluation point of a beam-shaping assembly.

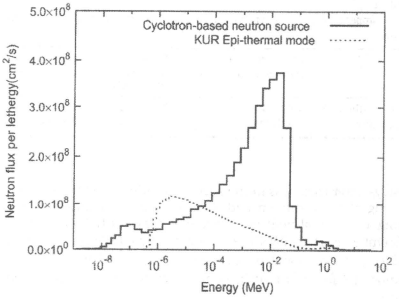

Fig. 6. Comparison with neutron spectrum at a gamma shield for KUR and CBNS.

In order to help the patient to take a comfortable irradiation position, an irradiation bed can be moved from right to left, or up and down, or back and forth. The irradiation bed and collimator can also be moved back; before switching on the treatment irradiation, the irradiation area can be confirmed by a view taken from the beam direction through the collimator aperture.

Further, so as to accurately set the patient in the position determined by the treatment planning system, an X-ray tube and an imaging plate are installed. The irradiation position is determined by comparing a bone image obtained by treatment planning (reconstructed by CT images) and the X-ray image of the imaging plate. The pair of X-ray tube and imaging plate can be moved to the neutron beam side and an image of the "beam's eye view" can be obtained. Laser markers are also installed; the irradiation position was set by the marking on the skin.

2.2. Reactor-based neutron source

2.2.1. Kyoto University Reactor (KUR)

KUR is a light-water-moderated, tank-type nuclear research reactor with a nominal power of 5 MW. It has been widely utilized for several research fields in various subject areas such as physics, chemistry, biology, engineering, agriculture, medicine, etc. since the first criticality in June 1964.

2.2.2. Heavy-water neutron irradiation facility (HWNIF)

HWNIF is a medical facility installed in KUR. The details of this facility are described in reference [11]. Fig. 5 shows schematic layout of HWNIF. The high-energy neutrons produced by fission reactions in core are moderated by the epithermal-neutron moderator, which is a mixture of aluminum and heavy-water ($Al:D_2O$ = 80%:20% in volume). A heavy-water spectrum shifter is installed outside of the epithermal-neutron moderator. The total heavy-water thickness can be changed from 0 to 90 cm in 10-cm increments for changing to various neutron spectrums. Thermal-neutron filters made of cadmium and boral are installed outside of the spectrum shifter, for the regulation of the thermal-neutron component and the formation of epithermal neutrons. Outside of these filters, a bismuth layer is placed for gamma-ray elimination. In this facility, neutron beams with various energy spectra from almost pure thermal to epithermal are obtained by controlling the

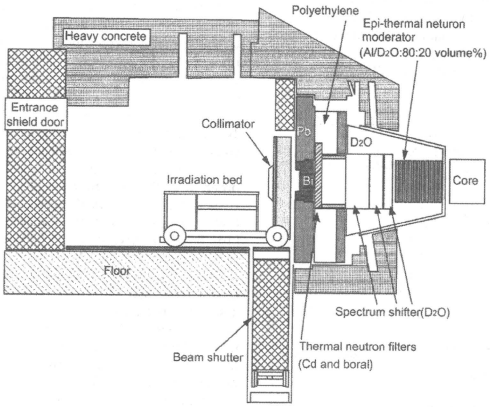

Fig. 5. Schematic layout of HWNIF at KUR.